Composites Part B 178 (2019) 107466

Contents lists available at ScienceDirect

Composites Part B

journal homepage: www.elsevier.com/locate/compositesb

Improved wave-transparent performances and enhanced mechanical properties for fluoride-containing PBO precursor modified cyanate ester resins and their PBO fibers/cyanate ester composites

Zheng Liu [a,1], Junliang Zhang [a,c,1], Lin Tang [a], Yuxiao Zhou [a], Yuhan Lin [a], Ruting Wang [b], Jie Kong [a], Yusheng Tang [a,**], Gu Junwei [a,b,*]

[a] MOE Key Laboratory of Material Physics and Chemistry Under Extraordinary Conditions, Shaanxi Key Laboratory of Macromolecular Science and Technology, Department of Applied Chemistry, School of Science, Northwestern Polytechnical University, Xi'an, Shaanxi, 710072, PR China
[b] Queen Mary University of London Engineering School, Northwestern Polytechnical University, Xi'an, Shaanxi, 710072, PR China
[c] School of Materials Science and Engineering, Henan University of Science and Technology, Luoyang, 471023, PR China

ARTICLE INFO

Keywords:
Cyanate ester (CE) resins
Fluoride-containing epoxy-terminated PBO precursor
PBO fibers
Interfacial bonding strength

ABSTRACT

Poly(*p*-phenylene-2,6-benzobisoxazole) (PBO) fibers can be applied as reinforcement to fabricate PBO/cyanate ester (CE) resin laminated composites with light weight, high specific strength & modulus, excellent dielectric properties, and extraordinary excellent thermal & humidity resistance for radome application. However, the surface of PBO fibers is extremely inert, resulting in poor interfacial compatibility to CE matrix. Besides, the toughness and wave-transparent performances of the cured CE resins need to be further improved. In this work, 2, 2-bis(3-amino-4-hydroxyphenyl) hexafluoropropane (6FAP) and terephthaloyl chloride (TPC) were performed to synthesize fluorine-containing epoxy-terminated PBO precursor (epoxy-*pre*FPBO) *via* condensation reaction followed by end-group functionalization with glycidol. Afterwards, epoxy-*pre*FPBO modified CE resins (FPBO-*co*-BADCy resins) were prepared by copolymerization of epoxy-*pre*FPBO and bisphenol A cyanate ester (BADCy). FPBO-*co*-BADCy resins with 7 wt% epoxy-*pre*FPBO displayed the optimal wave-transparent performances and mechanical properties. Dielectric constant (ε) and dielectric loss ($\tan\delta$) is respectively 2.48 and 0.0081, and the corresponding transmittance ($|T|^2$) at 10 MHz is 94.9%, higher than that of pure BADCy (92.7%). The corresponding flexural and impact strength was enhanced to 119.9 MPa and 12.3 kJ/m^2, 21.4% and 24.5% higher than that of pure BADCy, respectively. In addition, FPBO-*co*-BADCy resins presented better interfacial bonding strength with PBO fibers than that of pure BADCy.

1. Introduction

Poly(*p*-phenylene-2,6-benzobisoxazole) (PBO) fibers have relatively low density (1.56 g/cm^3), ultra-low dielectric constant (ε, 3.0) & dielectric loss ($\tan\delta$, 0.001), superior tensile strength (5.8 GPa) & modulus (270 MPa), and outstanding thermal resistance (T_{dmax} = 650 °C) in comparison with those of glass fibers [1,2], quartz fibers [3], and/or Kevalr fibers [4], *etc*. Therefore, PBO fibers have attracted significant attention in the preparation of high-performance wave-transparent/load integrated polymer matrix composites [5–7]. However, the weak interfacial compatibility between PBO fibers and polymer matrix always leads to poor mechanical properties, especially for interlaminar shear strength (ILSS) [8–10]. To our knowledge, different methods have been developed for the surface functionalization of PBO fibers, for instance, electrostatic adsorption [11], corona discharge [12], plasma [13–15], and radiation [16,17], *etc*. However, these approaches might usually damage the mechanical properties of the PBO fibers themselves and are difficult to industrialize as well [18,19].

Utilizing interfacial compatibilizer can effectively avoid the damage to surface structure of the reinforced fibers themselves, and such

* Corresponding author. MOE Key Laboratory of Material Physics and Chemistry Under Extraordinary Conditions, Shaanxi Key Laboratory of Macromolecular Science and Technology, Department of Applied Chemistry, School of Science, Northwestern Polytechnical University, Xi'an, Shaanxi, 710072, PR China.
** Corresponding author.
E-mail addresses: tys@nwpu.edu.cn (Y. Tang), gjw@nwpu.edu.cn, nwpugjw@163.com (J. Gu).
[1] The authors Zheng Liu and Junliang Zhang contributed equally to this work and should be considered *co*-first authors.

https://doi.org/10.1016/j.compositesb.2019.107466
Received 14 August 2019; Received in revised form 16 September 2019; Accepted 18 September 2019
Available online 18 September 2019

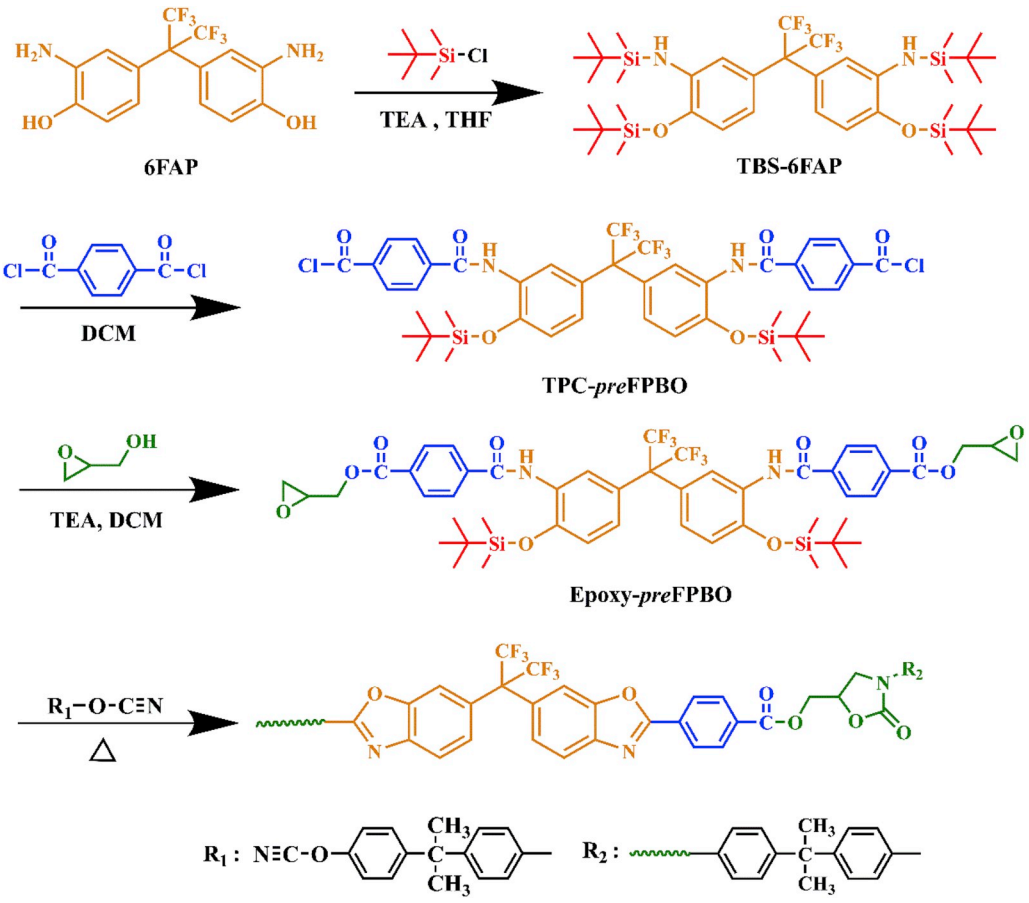

Scheme 1. Schematic diagram of synthesis for epoxy-*pre*FPBO and its reaction with BADCy matrix.

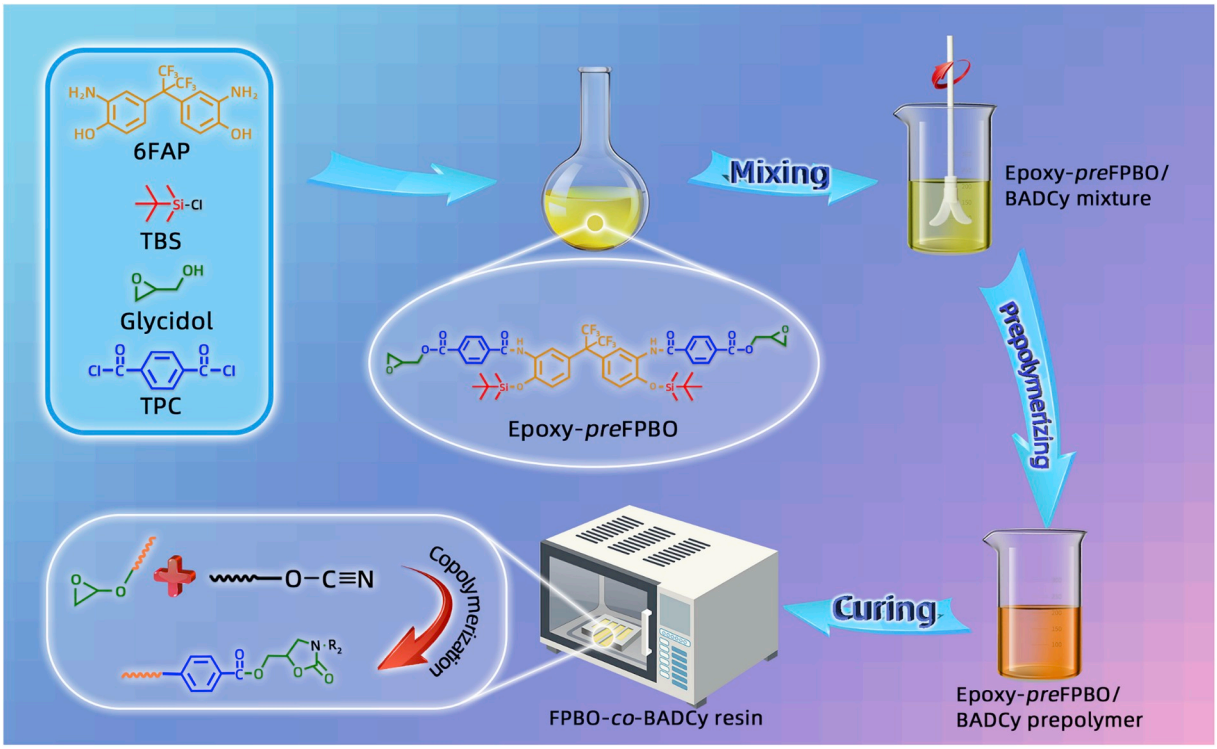

Fig. 1. Schematic diagram of preparation flow chart for FPBO-*co*-BADCy resin.

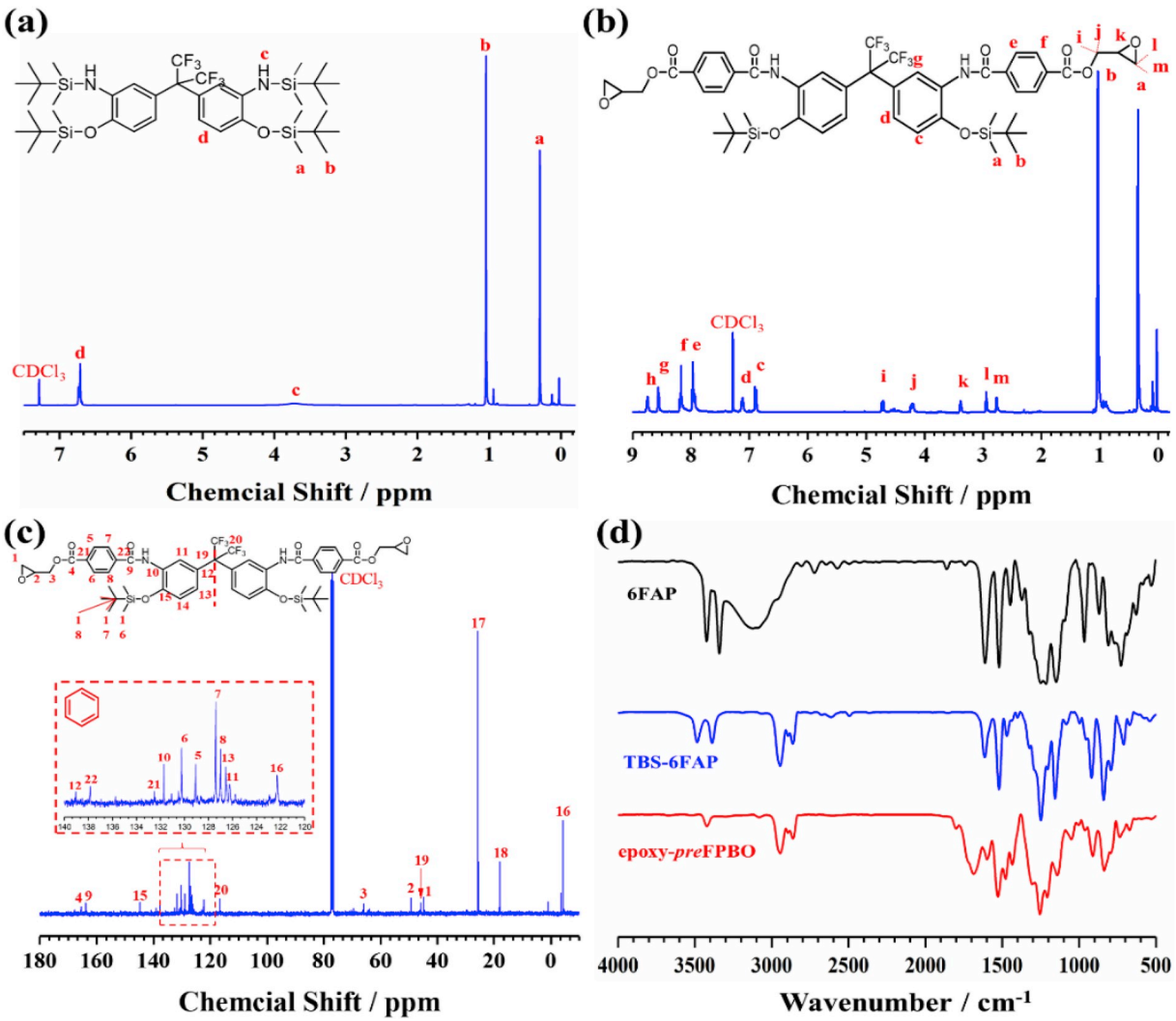

Fig. 2. (a)^{1}H NMR spectrum of TBS-6FAP; (b) ^{1}H NMR and (c) ^{13}C NMR spectra of epoxy-*pre*FPBO; (d) FTIR spectra of 6FAP, TBS-6FAP and epoxy-*pre*FPBO.

approach can also be applied in the lage-scale industrialized fabrication for polymer matrix composites [20–22]. Saves [23] et al. reported that the interfacial bonding between the high density polyethylene matrix and carbon fibers was significantly improved by using three different compatibilizers. In our previous work [24], novel PBO-*co*-BADCy resins were fabricated *via* copolymerization of epoxy-terminated PBO precursor (epoxy-*pre*PBO) and bisphenol A cyanate ester (BADCy). Compared with that of PBO fibers/BADCy composites, the obtained ε (2.86) and tanδ (0.0061) value of the PBO fibers/PBO-*co*-BADCy wave-transparent laminated composites was reduced by 14.4% and 59.1%, respectively, and the corresponding ILSS and flexural strength was also increased by 20.1% and 7.8%, respectively.

Compared with other polymer matrix, *e.g.* unsaturated polyester [25,26], polyoxymethylene [27], epoxy resin [28,29], and bismaleimide resin [30], cyanate ester (CE) resins are endowed with lower ε (2.8–3.2) and tanδ (0.002–0.008), and present better stability at different temperatures and frequencies, which are recognized as the optimal polymer matrix for next-generation of polymer matrix wave-transparent composites [31–33]. However, pure cured CE resins always suffer from poor toughness. Besides, the dielectric properties of cured CE resins are still unable to meet the real application requirements of full-band and high-performance radome systems [34,35]. Therefore, it is highly desirable to modify CE resins, in order to reduce the ε and tanδ values and synchronously increase the mechanical properties. He [36] et al. incorporated DOPO-HQ into BADCy resins, and the obtained modified BADCy resins presented excellent dielectric properties, with ε and tanδ value being 2.69 and 0.007, respectively.

Fluoropolymers possess ultra-low ε due to the fluorine or fluorine-containing groups in the molecular structure [37,38]. It is therefore possible to reduce ε and tanδ values of the polymers by attaching fluorine-containing groups to polymer backbone or side chain [39–41]. Wang [42] et al. prepared modified epoxy resin (DGEBF/DGEBA) containing trifluoromethyl (-CF_3) in the side chain *via* alkylation using 2, 2-bis(4-hydroxyphenyl)-hexafluoropropane and epichlorohydrin. The corresponding ε value of the DGEBF/DGEBA was reduced to 2.0, much lower than that of unmodified epoxy resin (3.8). In our previous work [43], synthesized 2-((3-(trifluoromethyl)phenoxy)methyl)oxirane (TFMPMO) was applied to modify BADCy *via* copolymerization. Compared with that of pure BADCy, BADCy resin modified with 15 wt% TFMPMO displayed relatively lower ε (2.75) and tanδ (0.0067), and significantly improved mechanical properties.

In this work, a new strategy for the fabrication of a new type interfacial compatibilizer, fluoride-containing epoxy-terminated PBO precursor (epoxy-preFPBO), was presented. Fluorine groups in epoxy-*pre*FPBO might reduce the ε and tanδ values of the BADCy matrix, and the epoxy groups can form oxazolinone, which would decrease the rigidity of cured BADCy. In addition, PBO-like structures (formed during the curing process of modified BADCy matrix [24,44]) can improve the interfacial compatibility between BADCy matrix and PBO fibers, which will be beneficial to the improvement of the ILSS of the final laminated

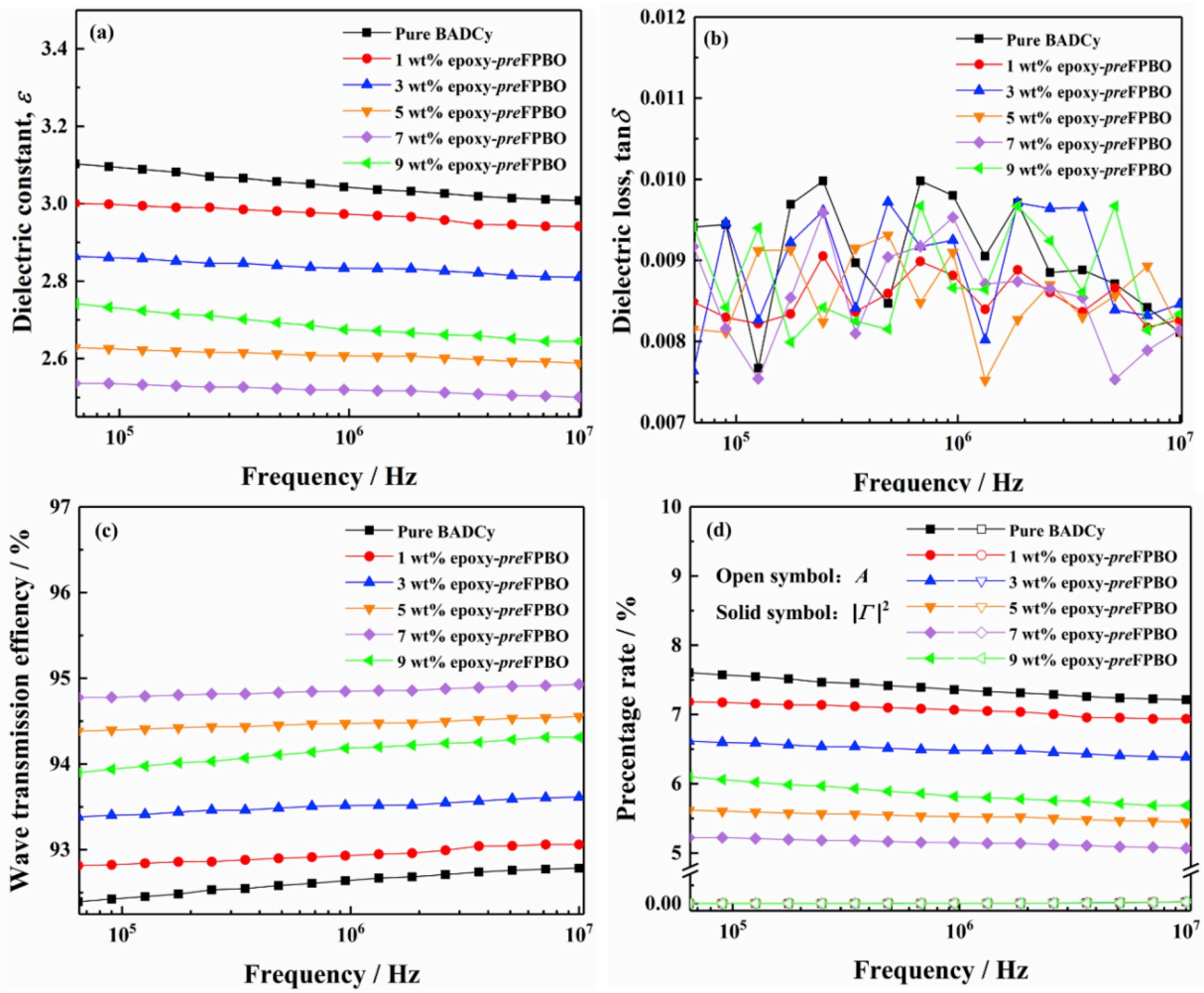

Fig. 3. Effects of epoxy-*pre*FPBO contents on the ε (a) and tanδ (b) values of the FPBO-*co*-BADCy resins at different testing frequencies; Wave transmission efficiency (c); Energy loss and reflection coefficient (d).

composites. Herein, epoxy-*pre*FPBO, synthesized from 2, 2-bis(3-amino-4-hydroxyphenyl)hexafluoropropane (6FAP) and terephthaloyl chloride (TPC) through condensation and end-group functionalization, was performed to modify BADCy resins (FPBO-*co*-BADCy resins) *via* copolymerization. Nuclear magnetic resonance (NMR) and fourier transform infrared (FTIR) were performed to analyze and characterize the obtained product structure. Furthermore, the effects of the epoxy-*pre*FPBO content on the dielectric & mechanical properties, thermal and water resistances of the FPBO-*co*-BADCy, and the interfacial compatibility (interfacial bonding strength) between PBO fibers and BADCy matrix were all investigated.

2. Experimental

2.1. Main materials

Detailed information can be found in **Supporting Information S1**.

2.2. Synthesis of epoxy-preFPBO

Epoxy-*pre*FPBO was synthesized referring to our previous published work [24]. Silane-protected 6FAP (TBS-6FAP) was firstly synthesized from 6FAP and tert-butyldimethylsilyl chloride, which was then reacted with TPC to obtain the fluorine-containing PBO precursor (TPC-*pre*FPBO). Finally, TPC-*pre*FPBO was reacted with glycidol to afford the fluorine-containing epoxy-terminated PBO precursor (epoxy-*pre*FPBO), as illustrated in Scheme 1. And the detailed synthetic procedures can be found in **Supporting Information S2**.

2.3. Fabrication of FPBO-co-BADCy resin

As displayed in Fig. 1, appropriate amount of epoxy-*pre*FPBO was dissolved in DMF and stirred uniformly under ultrasonic condition. BADCy was then added into the above solution and heated to 150 °C while stirring. Then the obtained mixture was kept reaction at 150 °C for 45 min to remove DMF. Finally, the above mixture was poured into a preheated mould, degassed in vacuum oven, and cured according to the following procedure of 180 °C/2 h + 200 °C/6 h + 220 °C/2 h.

2.4. Characterization

Detailed characterization methods can be found in **Supporting Information S3**.

3. Results and discussion

3.1. Structural characterization on TBS-6FAP and epoxy-preFPBO

Fig. 2 shows the ^{1}H NMR spectra of TBS-6FAP (a) and epoxy-*pre*FPBO (b), ^{13}C NMR spectrum of epoxy-*pre*FPBO (c), and FTIR spectra of 6FAP, TBS-6FAP, and epoxy-*pre*FPBO (d). In Fig. 2(a), the chemical shifts at 0.26, 1.04, 3.83, and 6.71 ppm correspond to the protons for -Si(CH_3)$_2$-,

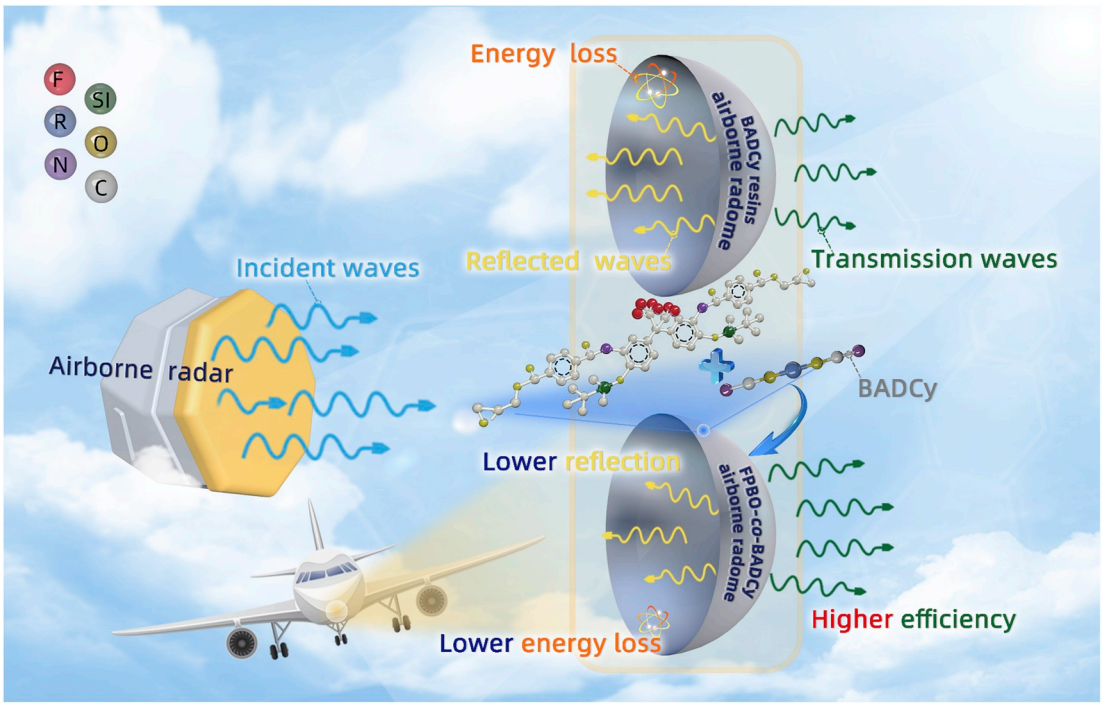

Fig. 4. Schematic diagram of electromagnetic waves transmission mechanism for FPBO-*co*-BADCy resins.

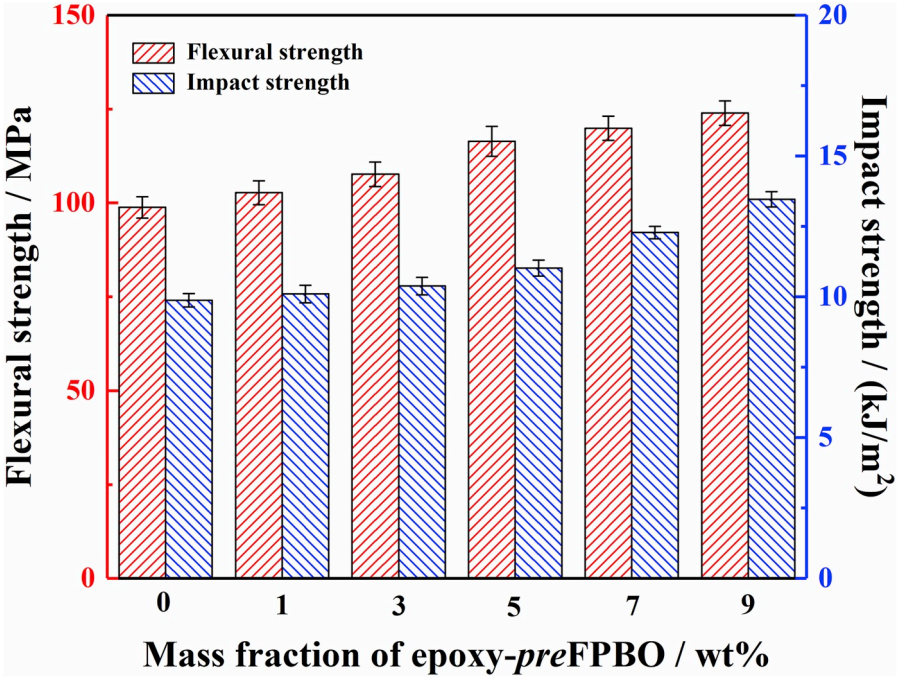

Fig. 5. Effects of epoxy-*pre*FPBO contents on the mechanical properties of the FPBO-*co*-BADCy resins.

–$C(CH_3)_3$-, –NH–Si-, and benzene, respectively. And the ratio of the integration for these peaks (peaks a, b, c, and d) was 12.32:17.84:1.00:3.05, which is consistent with the chemical formula of the product. In Fig. 2(b), the chemical shift at 8.74 ppm corresponds to the secondary amine (–NH–), which shifts to the lower field compared with that of TBS-6FAP. This was caused by the electron withdrawing effect of the carbonyl group in the amide group, which indicates that TPC has reacted with TBS-6FAP *via* condensation. The signals at 8.56, 7.14, and 6.97 ppm are attributed to the three protons with different chemical environment in the benzene ring of 6FAP. The peaks at chemical shifts of 8.23 and 7.97 ppm are ascribed to the protons of the benzene ring in TPC. In addition, a few more peaks appear at 2–5 ppm, corresponding to the glycidol. The ratio of the integration for these peaks (a:b:c:d:e:f:g:h:i:j:k:l:m in Fig. 2(b)) is 7.79:11.68:1.29:1.23:2.20:1.94:1.00:0.98:0.81:0.83:0.76:0.78:0.88, which is in good agreement with the structure of epoxy-*pre*FPBO. Besides, the ^{13}C peaks in Fig. 2(c) confirm all the carbon atoms of epoxy-*pre*FPBO. Meanwhile, in Fig. 2(d), compared to the spectrum of 6FAP, the disappearance of the hydroxyl and primary amine peaks at 3000-3500 cm^{-1}, and the appearance of the -C-Si- peak at 1005 cm^{-1} and -C-

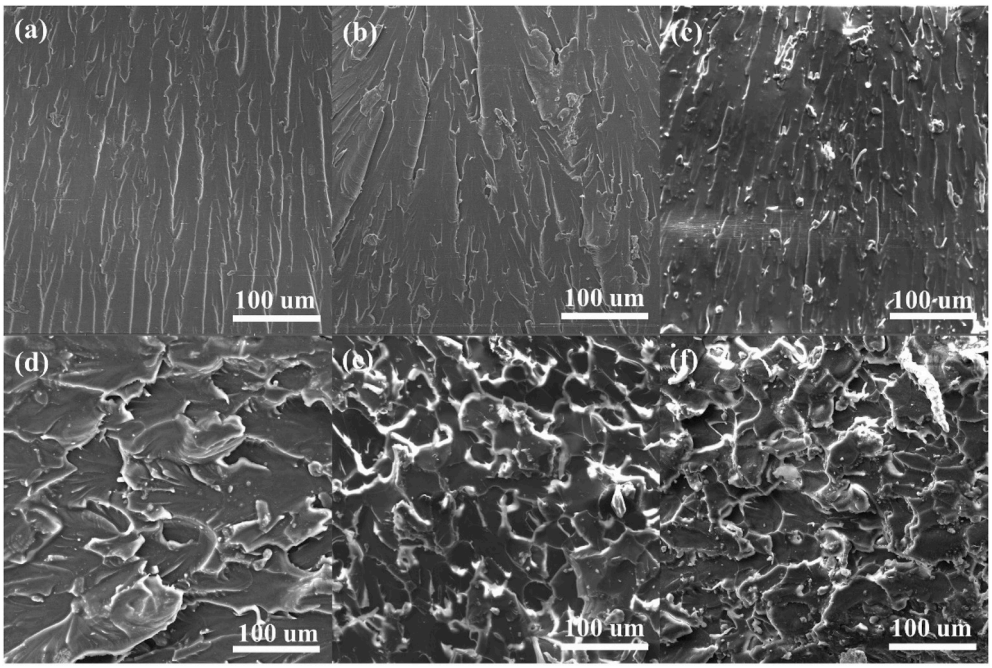

Fig. 6. SEM morphologies of impact fractures for FPBO-*co*-BADCy resins with different epoxy-*pre*FPBO content: (a) 0, (b) 1, (c) 3, (d) 5, (e) 7 and (f) 9 wt%.

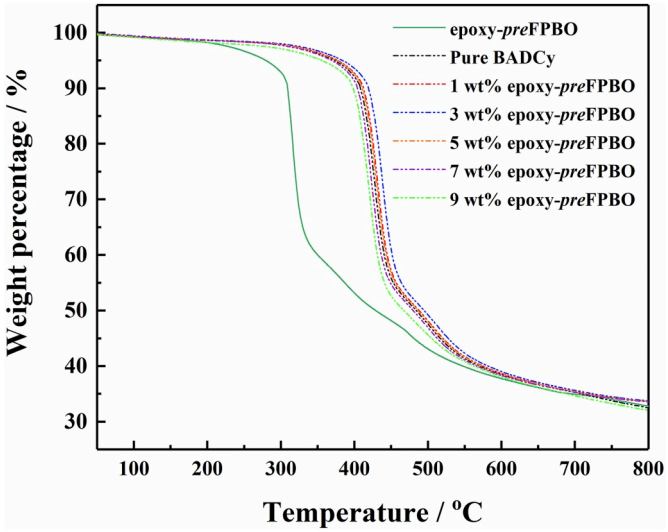

Fig. 7. TGA curves of epoxy-*pre*FPBO, pure BADCy and FPBO-*co*-BADCy resins.

O- peak at 1251 cm^{-1} of TBS-6FAP indicate the complete reaction between TBS and 6FAP. In addition, the characteristic peaks at 1000 and 1700 cm^{-1} is assigned to the epoxy group and carbonyl group, respectively, which suggests successful reaction between TPC and glycidol. Therefore, it can be deduced that the epoxy-*pre*FPBO has been synthesized successfully (For on-line FTIR spectra of FPBO-*co*-BADCy resins monitoring the curing process, see the **Supporting Information S4 and** Fig. S2).

3.2. Dielectric performances of the cured FPBO-co-BADCy

The amount of epoxy-*pre*FPBO affecting on the ε (a) and tanδ (b) values of the FPBO-*co*-BADCy at different frequencies are shown in Fig. 3. It can be observed that the ε value of the FPBO-*co*-BADCy resins decreases firstly before increases with increasing the amount of epoxy-*pre*FPBO. The ε value of FPBO-*co*-BADCy resins with 7 wt% epoxy-*pre*FPBO decreases to the minimum value of 2.48, lower than that of FPBO-*co*-BADCy resins with 9 wt% epoxy-*pre*FPBO (2.64). And the tanδ values of FPBO-*co*-BADCy resins stay in the relatively low range of 0.007–0.010 for all the analyzed contents.

The $-CF_3$ group (C–F bond) possesses low polarization and large free volume, which makes epoxy-*pre*FPBO present low ε. F atoms can reduce the electronic effects, in favor of decreasing the ε and tanδ values of the FPBO-*co*-BADCy resins. However, the epoxy groups in epoxy-*pre*FPBO can react with –OCN groups in BADCy to form the oxazolinone (presenting large polarization), and will partially replace the rigid triazine structures, resulting the increase of ε and tanδ values.

In addition, the relaxation time corresponding to various kinds of polarization is also different. The dipole polarization with a long relaxation time cannot keep up with the change of electric field, resulting in the decreased molecule polarization, presenting decreased ε value of the FPBO-*co*-BADCy resins with increasing the frequency.

For wave-transparent polymer composites, both the reflection of electromagnetic waves on the surface of dielectrics and the energy loss inside dielectrics belong to the loss of electromagnetic waves. The ratio of the above two losses can be measured by two parameters: reflection coefficient ($|\Gamma|^2$) and energy loss (A). The relationship between A, $|\Gamma|^2$ and the wave transmission ratio ($|T|^2$) of the dielectrics is shown in **Supporting Information S5**. According to equations S2-S4 and the actual testing condition, the $|T|^2$, $|\Gamma|^2$ and A curves of the FPBO-*co*-BADCy resins with different mass fraction of epoxy-*pre*FPBO at various frequencies are shown in Fig. 3(c) and (d). The $|T|^2$ of the FPBO-*co*-BADCy resins with 7 wt% epoxy-*pre*FPBO increases to 94.9% at 10 MHz, higher than that of pure BADCy matrix (92.7%). It can be seen that the $|T|^2$ of the FPBO-*co*-BADCy resins is inversely correlated with the ε and tanδ, and the $|\Gamma|^2$ is well above the A. Results suggest that the main way of energy loss of the electromagnetic waves for FPBO-*co*-BADCy resins is reflection loss, and decreasing ε value is beneficial to reducing the reflection loss, which will subsequently improve A. According to the impedance matching theory, if the impedance of the load phase matches that of transmission phase, no reflection occurs at the interface between the two phases during electromagnetic waves transmission [45]. The larger the ε value of the FPBO-*co*-BADCy resins, the bigger the impedance difference between the transport phase (air) and the load phase (FPBO-*co*-BADCy resins), resulting in the stronger interface reflection,

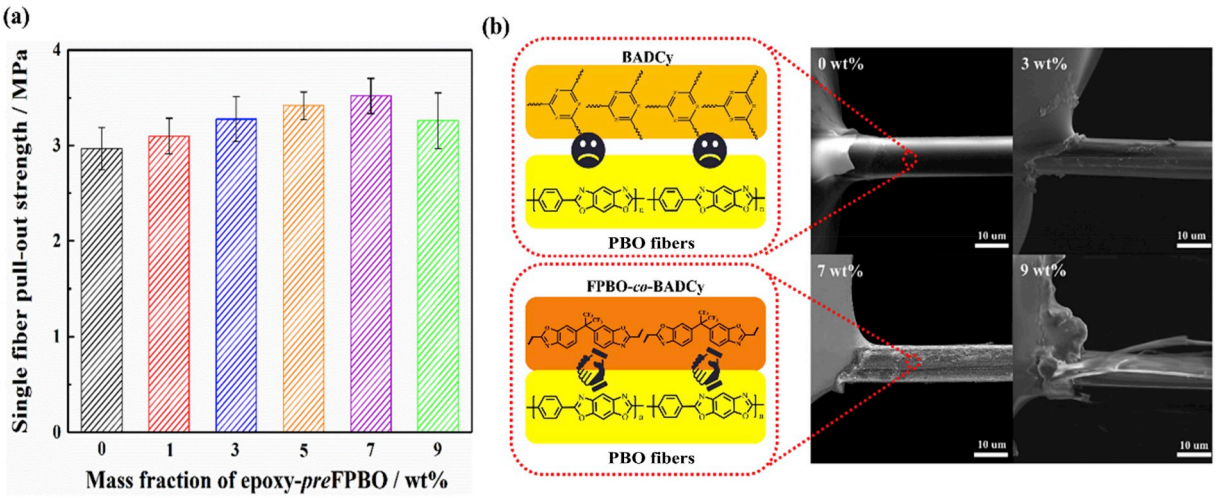

Fig. 8. (a) Single fiber pull-out strength of the PBO fibers/BADCy and PBO fibers/FPBO-*co*-BADCy micro-composites; (b) SEM images of the PBO fiber surfaces after single fiber pull-out test.

which reduces the final $|T|^2$ of the FPBO-*co*-BADCy resins (Transmission diagram is shown in Fig. 4).

3.3. Mechanical properties of cured FPBO-co-BADCy

Effects of the epoxy-*pre*FPBO content on the mechanical properties of the FPBO-*co*-BADCy resins are demonstrated in Fig. 5. Both the flexural strength and impact strength of the FPBO-*co*-BADCy resins gradually increase with increasing the mass fraction of epoxy-*pre*FPBO. Compared with that of pure BADCy matrix (flexural strength of 98.8 MPa and impact strength of 9.9 kJ/m^2), the corresponding flexural strength and impact strength of the FPBO-*co*-BADCy resins with 7 wt% epoxy-*pre*-FPBO are improved to 119.9 MPa and 12.3 kJ/m^2, increased by 21.4% and 24.5%, respectively.

On one hand, –CF_3 has large free volume, beneficial to the chain movement. On the other hand, the formed oxazolinone fragments (through the reaction of the epoxy groups in epoxy-*pre*FPBO with –OCN groups in BADCy [46]) in polycyanurate networks can decrease the rigidity of the networks as they increase the distance between crosslinks, which will reduce the flexural strength of the FPBO-*co*-BADCy resins. Besides, the additional copolymerization between epoxy and –OCN groups could reduce the curing temperature of BADCy, thus promoting the formation of the triazine, which will increase the crosslinking density and consequently improve the flexural strength. Herein, the latter plays a major role in the increasing of flexural strength for FPBO-*co*-BADCy resins. For the effects of F atoms on the water absorption of FPBO-*co*-BADCy resins, please see the **Supporting Information S6 and** Fig. S4. Fig. 6 shows the corresponding SEM morphologies of impact fractures for FPBO-*co*-BADCy resins. The impact fracture surface of pure BADCy matrix is relatively smooth, demonstrating a typical brittle feature. With increasing the amount of epoxy-*pre*FPBO, the roughness of impact fractures for the FPBO-*co*-BADCy resins and the degree of stress whitening gradually increase, beneficial for enhancing the impact toughness. These are consistent with those experimental results of the impact strength for FPBO-*co*-BADCy resins, as shown in Fig. 5.

3.4. Thermal properties of cured FPBO-co-BADCy

TGA curves of the epoxy-*pre*FPBO, pure BADCy, and FPBO-*co*-BADCy resins are shown in Fig. 7, and the corresponding characteristic thermal data are summarized in Table S2. The weight of epoxy-*pre*FPBO hardly changes below 200 °C owing to its relatively good thermal resistance. The maximum weight loss of epoxy-*pre*FPBO occurs between 250 °C and 350 °C, which can be attributed to the removal of the TBS structure during the thermal cyclization. The weight loss of epoxy-*pre*FPBO after 350 °C is mainly due to the destruction of the epoxy structure. Pure BADCy and FPBO-*co*-BADCy resins display less weight loss before 380 °C, owing to the better thermal resistance of a large number for crosslinked triazine in cured networks. The maximum weight loss of pure BADCy and FPBO-*co*-BADCy resins occur at around 400 °C, mainly attributed to the destruction of the triazine in pure BADCy and FPBO-*co*-BADCy resins.

The corresponding thermal decomposing temperatures of T_5 & T_{30}, and calculated $T_{Heat\text{-}resistance\ index}$ (T_{HRI}) values [47] of the FPBO-*co*-BADCy resins increase with increasing mass fraction of epoxy-*pre*FPBO and then decrease in comparison to that of pure BADCy. However, the variation of thermal resistance is marginal. The obtained T_{HRI} value of the FPBO-*co*-BADCy resins with 7 wt% epoxy-*pre*FPBO is 197.6 °C, slightly lower than that of pure BADCy (199.5 °C). To our knowledge, the T_{HRI} values can indicate the heat resistance, and the higher T_{HRI} value, the better heat resistance, it can be deduced that FPBO-*co*-BADCy resins still possess relatively excellent thermal stabilities. This is because the copolymerization between epoxy and –OCN groups could decrease the curing temperature of BADCy, thus causing the increase of the crosslinking density, in favor of enhancing the thermal stabilities. Besides, the addition of large amounts of epoxy groups probably destroys the regular structures of triazine, thus decreasing the crosslinking density of cured networks, which is against the thermal stabilities.

3.5. Interfacial compatibility of PBO fibers/FPBO-co-BADCy micro-composites

Fig. 8 demonstrates the contents of epoxy-*pre*FPBO affecting on the interfacial compatibility of PBO fibers and the FPBO-*co*-BADCy matrix, and the corresponding SEM images of the PBO fiber surfaces after single fiber pull-out test. As observed, the single fiber pull-out strength of the PBO fibers/FPBO-*co*-BADCy micro-composites increases to the maximum with increasing the amount of epoxy-*pre*FPBO and decreases afterwards. The maximum single fiber pull-out strength of the PBO fibers/FPBO-*co*-BADCy micro-composites with 7 wt% epoxy-*pre*FPBO is increased by 20.6% to 3.5 MPa from 2.9 MPa of PBO fibers/BADCy micro-composites.

The reason is that the interfacial compatibility between PBO fibers and BADCy resins is poor, therefore, the surface of PBO fibers for PBO fibers/BADCy micro-composites is smooth after single fiber pull-out test, and there is no residual BADCy resins on the surface of PBO fibers. With an optimum amount of added epoxy-*pre*FPBO, the residual FPBO-*co*-BADCy resins on the surface of PBO fibers gradually increase, mainly

attributed to the introduction of the PBO-like structure (formed during the curing process of modified BADCy resin [23,42]) in the interface of PBO fibers/FPBO-*co*-BADCy micro-composites, resulting in the improved interfacial compatibility, which is also in favor of enhancing interfacial adhesion between the PBO fibers and FPBO-*co*-BADCy matrix as illustrated in Fig. 8(b). However, the large number of added epoxy groups probably destroys the regular structures of triazine, causing the interface damage in the weakness of the FPBO-*co*-BADCy resins on the surfaces, finally against the corresponding single fiber pull-out strength.

4. Conclusions

In conclusion, a novel fluorine-containing epoxy-terminated PBO precursor (epoxy-*pre*FPBO) was synthesized, to successfully obtain the modified BADCy (FPBO-*co*-BADCy). The ε values of the FPBO-*co*-BADCy resins decreased firstly and then increased with increasing the amount of epoxy-*pre*FPBO, and the tanδ values of FPBO-*co*-BADCy resins stayed in the relatively low range of 0.007–0.010. The ε and tanδ values of FPBO-*co*-BADCy resins with 7 wt% epoxy-*pre*FPBO was respectively 2.48 and 0.0081, and the corresponding $|T|^2$ was 94.9%, better than that of pure BADCy (92.7%) at 10 MHz. Compared with that of pure BADCy matrix (flexural strength of 98.8 MPa and impact strength of 9.9 kJ/m^2), the flexural and impact strength of FPBO-*co*-BADCy resins with 7 wt% epoxy-*pre*FPBO was improved to 119.9 MPa and 12.3 kJ/m^2, increased by 21.4% and 24.5%, respectively. In addition, the FPBO-*co*-BADCy resins presented better interfacial bonding strength with PBO fibers than that of pure BADCy resins, as the single fiber pull-out strength increased to 3.5 MPa for PBO fiber/FPBO-*co*-BADCy micro-composites from 2.9 MPa for PBO fiber/BADCy micro-composites.

Declaration of interests

The authors declare that they have no known competing financial interests or personal relationships that could have appeared to influence the work reported in this paper.

Acknowledgements

This work is supported by Space Supporting Fund from China Aerospace Science and Industry Corporation (No. 2019-HT-XG); Foundation of Aeronautics Science Fund (Nos. 2016ZF03010 and 2015ZF53074); Fundamental Research Funds for the Central Universities (Nos. 310201911py010 and 310201911qd003); China Postdoctoral Science Foundation (No. 2019M653735); Open Fund from Henan University of Science and Technology; Y.H. Lin and R.T. Wang thank for the Undergraduate Innovation & Business Program in Northwestern Polytechnical University.

Appendix A. Supplementary data

Supplementary data to this article can be found online at https://doi.org/10.1016/j.compositesb.2019.107466.

References

[1] Godara A, Gorbatikh L, Kalinka G, Warrier A, Rochez O, Mezzo L, Luizi F, van Vuure AW, Lomov SV, Verpoest I. Interfacial shear strength of a glass fiber/epoxy bonding in composites modified with carbon nanotubes. Compos Sci Technol 2010;70(9):1346–52.
[2] He Y, Chen Q, Liu H, Zhang L, Wu D, Lu C, et al. Friction and wear of MoO3/graphene oxide modified glass fiber reinforced epoxy nanocomposites. Macromol Mater Eng 2019;304(8):1900166.
[3] Hatat-Fraile M, Liang R, Arlos MJ, He RX, Peng P, Servos MR, Zhou YN. Concurrent photocatalytic and filtration processes using doped TiO_2 coated quartz fiber membranes in a photocatalytic membrane reactor. Chem Eng J 2017;330:531–40.
[4] Tang L, Dang J, He M, Li J, Kong J, Tang Y, Gu J. Preparation and properties of cyanate-based wave-transparent laminated composites reinforced by dopamine/POSS functionalized Kevlar cloth. Compos Sci Technol 2019;169:120–6.
[5] Dai Y, Feng J, Meng C, Luo L, Liu X. Synthesis of a novel cross-linker with high reactivity for enhancing compressive strength of high-performance organic fibers. Chemicals 2019;4(13):3980–3.
[6] Hu Z, Shao Q, Huang Y, Yu L, Zhang D, Xu X, Lin J, Liu H, Guo Z. Light triggered interfacial damage self-healing of poly(p-phenylene benzobisoxazole) fiber composites. Nanotechnology 2018;29(18):185602.
[7] Shao Q, Hu Z, Xu X, Yu L, Zhang D, Huang Y. Mussel-inspired immobilization of BN nanosheets onto poly(p-phenylene benzobisoxazole) fibers: multifunctional interface for photothermal self-healing. Appl Surf Sci 2018;440:1159–65.
[8] Gu H, Xu X, Cai J, Wei S, Wei H, Liu H, et al. Controllable organic magnetoresistance in polyaniline coated poly(p-phenylene-2,6-benzobisoxazole) short fibers. Chem Commum 2019;55(68):10068–71.
[9] Hu Z, Lu F, Liu Y, Zhao L, Yu L, Xu X, Yuan W, Zhang Q, Huang Y. Construction of anti-ultraviolet "shielding clothes" on poly(p-phenylene benzobisoxazole) fibers: metal organic framework-mediated absorption strategy. ACS Appl Mater Interfaces 2018;10(49):43262–74.
[10] Luo L, Hong D, Zhang L, Cheng Z, Liu X. Surface modification of PBO fibers by direct fluorination and corresponding chemical reaction mechanism. Compos Sci Technol 2018;165:106–14.
[11] Zhu M, Ma J. Basalt fiber modified with lanthanum-ethylenediaminetetraacetic acid as potential reinforcement of cyanate matrix composites. Appl Surf Sci 2019;464:636–43.
[12] Chen L, Hu Z, Zhao F, Xing L, Jiang B, Huang Y. Enhanced interfacial properties of PBO fiber via electroless nickel plating. Surf Coat Technol 2013;235:669–75.
[13] Chen L, Wang C, Wu Z, Wu G, Huang Y. Atomic oxygen erosion behaviors of PBO fibers and their composite: microstructure, surface chemistry and physical properties. Polym Degrad Stab 2016;133:275–82.
[14] Jia C, Wang Q, Chen P, Lu S, Ren R. Wettability assessment of plasma-treated PBO fibers based on thermogravimetric analysis. Int J Adhesion Adhes 2017;74:123–30.
[15] Liu D, Chen P, Chen M, Yu Q, Lu C. Effects of argon plasma treatment on the interfacial adhesion of PBO fiber/bismaleimide composite and aging behaviors. Appl Surf Sci 2011;257(23):10239–45.
[16] Zhang C, Huang Y, Zhao Y. Surface analysis of γ-ray irradiation modified PBO fiber. Mater Chem Phys 2005;92(1):245–50.
[17] Wang P, Tang Y, Yu Z, Gu J, Kong J. Advanced aromatic polymers with excellent antiatomic oxygen performance derived from molecular precursor strategy and copolymerization of polyhedral oligomeric silsesquioxane. ACS Appl Mater Interfaces 2015;7(36):20144–55.
[18] Gu J, Li Y, Liang C, Tang Y, Tang L, Zhang Y, Kong J, Liu H, Guo Z. Synchronously improved dielectric and mechanical properties of wave-transparent laminated composites combined with outstanding thermal stability by incorporating iysozyme/POSS functionalized PBO fibers. J Mater Chem C 2018;6(28):7652–60.
[19] Lai X, Guo R, Xiao H, Lan J, Jiang S, Cui C, Qin W. Flexible conductive copper/reduced graphene oxide coated PBO fibers modified with poly(dopamine). J Alloy Comp 2019;788:1169–76.
[20] Kaldéus T, Träger A, Berglund LA, Malmström E, Lo Re G. Molecular engineering of the cellulose-poly(caprolactone) bio-nanocomposite interface by reactive amphiphilic copolymer nanoparticles. ACS Nano 2019;13(6):6409–20.
[21] Rana AK, Mandal A, Bandyopadhyay S. Short jute fiber reinforced polypropylene composites: effect of compatibiliser, impact modifier and fiber loading. Compos Sci Technol 2003;63(6):801–6.
[22] Zhang L, Deng H, Jing Y, Tao L, Fu Q. An effective compatibilizer for tin fluorophosphate glass/polymer composites obtained from "one pot" KF-RAFT polymerization. Compos Sci Technol 2018;168:336–45.
[23] Savas LA, Tayfun U, Dogan M. The use of polyethylene copolymers as compatibilizers in carbon fiber reinforced high density polyethylene composites. Compos B Eng 2016;99:188–95.
[24] Gu J, Dong W, Xu S, Tang Y, Ye L, Kong J. Development of wave-transparent, lightweight composites combined with superior dielectric performance and desirable thermal stabilities. Compos Sci Technol 2017;144:185–92.
[25] Chen X, Li K, Zheng S, Fang Q. A new type of unsaturated polyester resin with low dielectric constant and high thermostability: preparation and properties. RSC Adv 2012;2(16):6504–8.
[26] Triki A, Guicha M, Ben Hassen M, Arous M, Fakhfakh Z. Studies of dielectric relaxation in natural fibres reinforced unsaturated polyester. J Mater Sci 2011;46(11):3698–707.
[27] Yang J, Yang W, Wang X, Dong M, Liu H, Wujcik EK, et al. Synergistically toughening polyoxymethylene by methyl methacrylate–butadiene–styrene copolymer and thermoplastic polyurethane. Macromol Chem Phys 2019;220(12):1800567.
[28] Choi I, Kim JG, Lee DG, Seo IS. Aramid/epoxy composites sandwich structures for low-observable radomes. Compos Sci Technol 2011;71(14):1632–8.
[29] Zhao M, Meng L, Ma L, Ma L, Yang X, Huang Y, Ryu JE, Shankar A, Li T, Yan C, Guo Z. Layer-by-layer grafting CNTs onto carbon fibers surface for enhancing the interfacial properties of epoxy resin composites. Compos Sci Technol 2018;154:28–36.
[30] Han X, Yuan L, Gu A, Liang G. Development and mechanism of ultralow dielectric loss and toughened bismaleimide resins with high heat and moisture resistance based on unique amino-functionalized metal-organic frameworks. Compos B Eng 2018;132:28–34.
[31] Guan Q, Yuan L, Zhang Y, Gu A, Liang G. Improving the mechanical, thermal, dielectric and flame retardancy properties of cyanate ester with the encapsulated epoxy resin-penetrated aligned carbon nanotube bundle. Compos B Eng 2017;123:81–91.

[32] He J, Hou D, Ma H, Li X, Li D. Preparation of phosphorus-containing cyanate resin with low curing temperature while excellent flame resistance and dielectric properties. J Macromol Sci 2019;56(7):629–39.
[33] Zhang Z, Xu W, Yuan L, Guan Q, Liang G, Gu A. Flame-retardant cyanate ester resin with suppressed toxic volatiles based on environmentally friendly halloysite nanotube/graphene oxide hybrid. J Appl Polym Sci 2018;135(31):46587.
[34] Zhang Y, Jia C. High-performance cyanate ester composites with plasma-synthesized $MgSiO_3$-SiO_2-hBN powders for thermally conductive and dielectric properties. Ceram Int 2019;45(5):6491–8.
[35] Zheng L, Yuan L, Guan Q, Liang G, Gu A. High-k 3D-barium titanate foam/phenolphthalein poly(ether sulfone)/cyanate ester composites with frequency-stable dielectric properties and extremely low dielectric loss under reduced concentration of ceramics. Appl Surf Sci 2018;427:1046–54.
[36] He J, Hou D, Ma H, Li X, Li D. Preparation of phosphorus-containing cyanate resin with low curing temperature while excellent flame resistance and dielectric properties. J Macromol Sci 2019;56(7):629–39.
[37] Song N, Yao H, Ma T, Wang T, Shi K, Tian Y, Zhang B, Zhu S, Zhang Y, Guan S. Decreasing the dielectric constant and water uptake by introducing hydrophobic cross-linked networks into co-polyimide films. Appl Surf Sci 2019;480:990–7.
[38] Tao Z, Yang S, Ge Z, Chen J, Fan L. Synthesis and properties of novel fluorinated epoxy resins based on 1,1-bis(4-glycidylesterphenyl)-1-(3′-trifluoromethylphenyl)-2,2,2-trifluoroethane. Eur Polym J 2007;43(2):550–60.
[39] Zhou J, Fang L, Wang J, Sun J, Jin K, Fang Q. Post-functionalization of novolac resins by introducing thermo-crosslinkable –OCF=CF2 groups as the side chains: a new strategy for production of thermosetting polymers without releasing volatiles. Polym Chem 2016;7(26):4313–6.
[40] Shaver AT, Yin K, Borjigin H, Zhang W, Choudhury SR, Baer E, Mecham SJ, Riffle JS, McGrath JE. Fluorinated poly(arylene ether ketone)s for high temperature dielectrics. Polymer 2016;83:199–204.
[41] Tian S, Sun J, Jin K, Wang J, He F, Zheng S, Fang Q. Postpolymerization of a fluorinated and reactive poly(aryl ether): an efficient way to balance the solubility and solvent resistance of the polymer. ACS Appl Mater Interfaces 2014;6(22):20437–43.
[42] Wang JY, Yang SY, Huang YL, Tien HW, Chin WK, Ma CCM, Shu WJ. Synthesis and properties of trifluoromethyl groups containing epoxy resins cured with amine for low D_k materials. J Appl Polym Sci 2012;124(3):2615–24.
[43] Gu J, Dong W, Tang Y, Guo Y, Tang L, Kong J, Tadakamalla S, Wang B, Guo Z. Ultralow dielectric, fluoride-containing cyanate ester resins with improved mechanical properties and high thermal and dimensional stabilities. J Mater Chem C 2017;5(28):6929–36.
[44] Zhang K, Han L, Froimowicz P, Ishida H. A smart latent catalyst containing o-trifluoroacetamide functional benzoxazine: precursor for low temperature formation of very high performance polybenzoxazole with low dielectric constant and high thermal stability. Macromolecules 2017;50(17):6552–60.
[45] Wang Lei, Chen Lixin, Song Ping, Liang Chaobo, Lu Yuanjin, Qiu Hua, Zhang Yali, Kong Jie, Gu Junwei. Fabrication on the annealed $Ti_3C_2T_x$ MXene/Epoxy nanocomposites for electromagnetic interference shielding application. Compos B Eng 2019;171:111–8.
[46] Zhang X, Gu A, Liang G, Zhuo D, Yuan L. Liquid crystalline epoxy resin modified cyanate ester for high performance electronic packaging. J Polym Res 2011;18(6):1441–50.
[47] Gu J, Lv Z, Wu Y, Guo Y, Tian L, Qiu H, Li W, Zhang Q. Dielectric thermally conductive boron nitride/polyimide composites with outstanding thermal stabilities via in-situ polymerization-electrospinning-hot press method. Composites Part A 2017;94:209–16.